Wavelet Filtering of Signals without Using Model Functions

Yu. K. Taranenko[1*] and N. Rizun[2**]

[1]*Private Enterprise Likopak, Dnipro, Ukraine*
[2]*Gdansk University of Technology, Gdansk, Poland*
ORCID: 0000-0003-2209-2244, e-mail: tatanen@ukr.net
ORCID: 0000-0002-4343-9713, e-mail: nina.rizun@pg.edu.pl

Abstract—The effective wavelet filtering of real signals is impossible without determining their shape. The shape of a real signal is related to its wavelet spectrum. For shape analysis, a continuous color wavelet spectrogram of signal level is often used. The disadvantage of continuous wavelet spectrogram is the complexity of analyzing a blurry color image. A real signal with additive noise strongly distorts the spectrogram based on continuous wavelet analysis compared to a pure signal. Therefore, the identification of a real signal by using a continuous color wavelet spectrogram is difficult. To solve this problem, for the first time, a comparative analysis of spectrograms of signals and correlation matrices is carried out. The spectrograms of signals are obtained based on continuous wavelet transformation in the form of images with areas of different colors of variable intensity. Correlation matrices are computed by using mathematical functions of the coefficients of discrete wavelet spectra.

COMMON NOTATIONS

Discrete wavelets: bior1.1, bior1.3, bior1.5, bior2.2, bior2.4, bior2.6, bior2.8, bior3.1, bior3.3, bior3.5, bior3.7, bior3.9, bior4.4, bior5.5, bior6.8, coif1, coif2, coif3, coif4, coif5, coif6, coif7, coif8, coif9, coif10, coif11, coif12, coif13, coif14, coif15, coif16, coif17, db1, db2, db3, db4, db5, db6, db7, db8, db9, db10, db11, db12, db13, db14, db15, db16, db17, db18, db19, db20, db21, db22, db23, db24, db25, db26, db27, db28, db29, db30, db31, db32, db33, db34, db35, db36, db37, db38, dmey, haar, rbio1.1, rbio1.3, rbio1.5, rbio2.2, rbio2.4, rbio2.6, rbio2.8, rbio3.1, rbio3.3, rbio3.5, rbio3.7, rbio3.9, rbio4.4, rbio5.5, rbio6.8, sym2, sym3, sym4, sym5, sym6, sym7, sym8, sym9, sym10, sym11, sym12, sym13, sym14, sym15, sym16, sym17, sym18, sym19, sym20.

1. INTRODUCTION

The effectiveness of methods for denoising of signals is determined by the nature of the signal itself, and a limited nature of noises – mainly the white uncorrelated noise with zero mathematical expectation. Therefore, the first and crucial stage is the signal identification using any filtering method. The basics of signal identification are given in [1].

In this work, trivial but critical remarks are made about the fact that any signal is characterized by its shape. After the quantization by level, the shape is determined by a set of instantaneous values and the distribution of time intervals for each quantization level. Many works are dedicated to the search for integral characteristics of the form. Among them, one can distinguish identifiers and classifiers based on machine learning, for example, using neural networks [2].

The main disadvantage of machine learning methods for signal identification is the fact that they are designed only for a specific group of signals, for example, electrocardiogram (ECG) signals. In addition, such algorithms have a low noise immunity and low performance. For further unification by the machine learning method in terms of signal identification and filtering, the analysis of spectral characteristics is considered to be promising [3].

From this summary of problems, one conclusion can be drawn, i.e., the stages of problem-solving should be as follows: signal identification, selection, and implementation of filtering, and only afterwards – the

classification methods. Therefore, let us move on to the substantive review of conventional and recursive Discrete Wavelet Transform (DWT) filtering methods.

2. LITERATURE BACKGROUND AND PROBLEM STATEMENT

Relatively recently, a paper [4] was published. To compare our results with those given in this publication, we shall study a numerical experiment in detail. The second-order recursive inverse (RI) adaptive algorithm used by the authors consists in decomposing a noisy signal into a filter bank, the output of which is converted into a group of coefficients by which the signal features are calculated. The signal is restored in a form close to the original non-noisy signal. The recursive least squares (RLS) algorithm can be implemented on any other principle of filtering. The difference is that the approach to the original signal is carried out by the least-squares method.

According to the numerical experiment, the R algorithm proposed by the authors of this publication is compared with the RLS algorithm under conditions of the uncorrelated white Gaussian noise with variance $\sigma^2 = 0.15$ and zero mathematical expectation. For the reproducibility of the results, 1000 realizations were carried out.

Subsequently, the following ratio for the correlated noise was obtained:

$$N_0(k+1) = 0{,}7 N_0(k) + \nu(k),$$

where $\nu(k)$ is the white Gaussian process with its mean value equal to zero and the variance which supports SNR = 30 dB. The convergence rate of the R algorithm to SNR = –30 dB is 850 iterations, which is 0.0035 dB per iteration. The noise level before filtering corresponds to SNR = 30.

Reconstruction of the signal obtained by the R algorithm is carried out according to the formula:

$$x(k) = \sum_{j=0}^{j-1} \sum_{n \in z} \theta_{j,n} \psi_{j,n}(k), \tag{1}$$

where $\theta_{j,n}$ are the wavelet coefficients, $\psi_{j,n}(k)$ are the wavelet functions that form an orthogonal basis.

We used a specifically generated signal written in a generalized form:

$$x_i(k) = 1{.}79 x_i(k-1) - 1{.}85 x_i(k-2) + 1{.}27 x_i(k-3) - 0{.}41 x_i(k-4) + n_0(k), \tag{2}$$

where $n_0(k)$ is the noise component.

The main disadvantage of the presented algorithm is that the filtering efficiency in terms of the mean squared error (MSE) indicator does not depend on the signal shape $x(k)$. Moreover, the recursive DWT is advisable to be applied when the minimum possible error is achieved by the direct method.

In this case, the performance indicator can be the ratio of the difference in decibels between

(i) the noise level in the MSE_2 signal filtered by the recursive method, and

(ii) the MSE_1 signal filtered by the direct method to the N number of iterations until the saturation is reached:

$$K = \frac{MSE_2 - MSE_1}{N}. \tag{3}$$

Now it is reasonable to consider the algorithm for achieving the minimum MSE or RMSE when identifying the signal after DWT filtering. One of such algorithms, namely the analysis of the effectiveness of the wavelet package for detecting the specific ultrasonic signals, is considered in publication [5]. This paper discusses the Batch Wavelet Transform (BWT) method for decomposing and reconstructing an ultrasonic signal reflected from C30 concrete grade with simultaneous noise suppression.

To analyze the performance of the proposed method, the following indicators are used:

1. Signal-to-noise ratio:

$$\text{SNR} = 10 \lg \left[\frac{\sum_{n=1}^{N} S(n)^2}{\sum_{n=1}^{N} (S(n) - X(n))^2} \right]. \tag{4}$$

2. Root-mean-square error (RMSE):

$$\text{RMSE} = \sqrt{\sum_{n=1}^{N} (X(n) - S(n))^2 / N}. \tag{5}$$

3. Pearson correlation coefficient (PCC):

$$\text{PCC} = \text{Cov}(X(n), S(n)) / \sigma_x \sigma_s. \tag{6}$$

4. Smoothness (SM):

$$\text{SM} = \frac{\sum_{n=1}^{N-1} [S(n+1) - S(n)]^2}{\sum_{n=1}^{N-1} [S(n+1) - X(n)]^2}. \tag{7}$$

In the above equations $X(n)$ is the original signal, $S(n)$ is the signal after the suppression, N is the signal length, σ_x and σ_s are the standard deviations of $X(n)$ and $S(n)$, $\text{Cov}(\cdot)$ — covariance function, respectively.

In the publication, ten signals were modeled according to the formula:

$$s(t) = \beta e^{-2(t-\tau)^2} \cos(2\pi f_s(t - \tau) + \varphi), \tag{8}$$

where $\beta = 1, \tau = 4, \varphi = 0, f_s = 5$.

The noise was added to the signal with SNR = 20 dB. After averaging, the following parameters were obtained: SNR = 11.1728 dB, RMSE = 0.0147, PCC = 0.9598, SM = 0.3344.

The disadvantage of this publication is its narrow focus on solving the particular problem of ultrasonic testing of concrete, which does not allow us to draw a conclusion about the BWT method is question.

A detailed description of the methods with the general and universal thresholds, which will be used by the authors of this paper as a zero recursion of signal, is presented in detail in [6]. The method without a threshold is described in [7].

The conducted literature review confirms the need for a detailed study of the possibilities of using the recursive method of discrete wavelet filtering to identify large groups of signals. The study should be carried out considering the use of literary data on the maximum efficiency of the known methods with the general and universal thresholds, as well as with the method without a threshold, such as zero recursion.

Increasing the efficiency of the given methods by using recursion is a highly urgent task. It will expand the application scope of DWT methods for a group of signals with a high degree of non-stationarity, for which this method has not been previously applied.

The purpose of this work is:

– to compare the selectivity of continuous (CWT) and discrete (DWT) wavelet transform methods for spectral analysis under Gaussian noise using an example of separating groups of signals close in spectrum;

– to determine the mathematical functions for processing wavelet coefficients to identify the signal by the spectrum for the DWT method based on the entropy of the signal;

– to develop recursive algorithms for DWT filtering of signals identified by the spectrum;

– to conduct a numerical and graphical comparative analysis of the developed filtering algorithms and the known DWT filtering methods taking into account the number of recursion cycles.

Table 1. Shapes and spectra of signals' power. Group 1
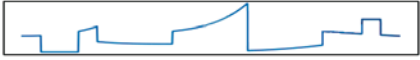
Signal	Forms of model signals	Wavelet power spectral density
Blocks		
Bumps		
Piece-polynomial		
Piece-regular		

Table 2. Shapes and spectra of signals' power. Group 2

Signal	Forms of model signals	Wavelet power spectral density
HiSine		
LoSine		

3. SELECTING SIGNALS FOR CWT AND DWT ANALYSIS

We will use the following types of signals [8]–[11]: blocks, bumps, heavisine (signal "heavy sinus"), doppler (doppler signal), ramp (sawtooth signal), hisine (signal function sin(0.6902$N\pi t$)), losine (signal function sin(0.3333$N\pi t$)), linchirp (signal with the linear frequency modulation), twochirp (signal with the double linear frequency modulation), quadchirp (signal with the square function of frequency versus time), mishmash (linchirp+quadchirp+hisine), wernersorrows (Werner signal), hypchirps (signal containing two frequencies with hyperbolic functions of time), linchirps (signal containing two frequencies with linear functions of time), chirps (sum of four signals with linear hyperbolic and square functions of frequency versus time), gabor (two modulated Gabor functions), sineoneoverx (sinusoidal signal with the frequency inversely proportional to time), piece-regular (normal pulse signal), piece-polynomial (piece-polynomial signal), riemann (Riemann non-differentiable function).

For visual assessment of proximity of spectrograms, we will use the software implementation import scalogram [12] with a high visual sensitivity to the features of signals.

4. CWT VISUAL SPECTRUM ANALYSIS

To build a scale diagram of the spectrum power, we use the representation of the Morlet (continuous) wavelet:

$$W(a,b) = \frac{\pi^{-1/4}}{\sqrt{a}} \int\limits_{-\infty}^{\infty} f(t)\exp\left(-i\omega_0 \frac{t-b}{a}\right)\exp\left(\frac{1}{2}\left(\frac{t-b}{a}\right)^2\right)dt, \qquad (9)$$
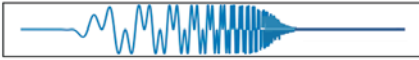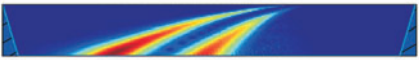
Table 3. Shapes and spectra of signals' power. Group 3
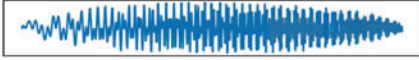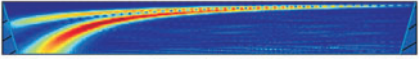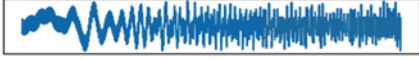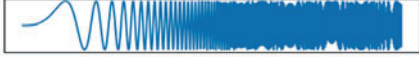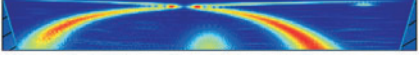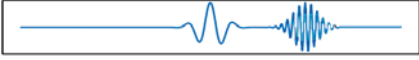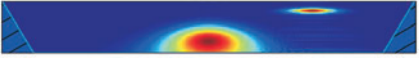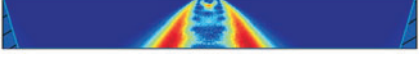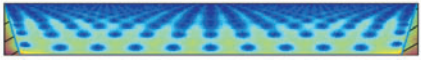
Signal	Forms of model signals	Wavelet power spectral density
HypChirps		
LinChirp		
LinChirps		
MishMash		
QuadChirp		
TwoChirp		
Chirps		

Table 4. Shapes and spectra of signals' power. Group 4
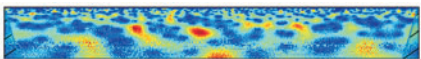
Signal	Forms of model signals	Wavelet power spectral density
Doppler		
Gabor		
HeaviSine		
Ramp		
SineOneOverX		

where a is scale, b is shift, $f(t)$ is the signal function, ω_0 is the frequency. Then local spectrum power is $|W(a, b)|^2$. Some shapes and spectra of signals are presented in Table 1. Tables 2–5 show signals similar in shape and spectrum.

Table 5. Shapes and spectra of signals' power. Group 5

Signal	Forms of model signals	Wavelet power spectral density
Riemann		
WernerSorrows		

The disadvantage of the analysis is the distortion of the image from noise ($m = 0$, $\sigma = 0.4$) in a real signal, for example,

Blocks		

Discrete pulses create cone-shaped structures on the spectrogram, also known as the cone of influence. The noise of the real signal destroys the cone of influence. Thus, the identification becomes impossible.

5. SYNTHESIS OF NOISE-RESISTANT CORRELATION MATRICES

The presented identification of groups of signals is carried out according to the method [13]. The disadvantage of this grouping is the subjectivity of the visual comparison of power spectra. In addition, it is impossible to identify real signals containing noise.

Correlation numerical analysis based on the DWT expansion allows the most accurate grouping of real signals by shape and spectral characteristics [14]. To build a correlation matrix with DWT signal transformation to achieve the maximum selectivity, the frequency subbands f_j of each level j must be mathematically processed by expanding $U_j = [f_{j1}, \dots, f_{jn}]$ by the functions to be selected.

The main function is the Shannon entropy, which can conditionally divide signals into simple and complex ones by comparing the numerical values of the entropy (Fig. 1).

As can be seen from Fig. 1, the noise has little effect on the Shannon entropy, which makes it possible to identify noisy signals, taking into account their complexity. On the graph, the dots almost lie on the broken line of the pure signal. Signals "Piece-Regular" and "Piece-Polynomial" are sharply distinguished by complexity from the rest. For these signals, as well as for signals Blocks, HeaviSine, MishMash, Chirps and WernerSorrows functions are used that determine the average value of the derivative, the frequency of the zero crossing, the average speed of the transition of a given signal amplitude. We denote these functions as f_{1-3}.

The remaining signals are conditionally simple, and their expansion coefficients DWT_j are processed by the functions of variance, standard deviation, mean value, 5th, 25th, 75th, 95th percentile, rms value, and squared rms amplitude. We denote these functions as f_{4-12}.

However, the above division is conditional, and with independent functions, their full set F works on the sensitivity of the matrix

$$F = f_{1-3} + f_{4-12}. \tag{10}$$

Apart from the choice of these functions, the wavelet has a strong effect on the selectivity of the correlation matrix, while the difference in the number of features before and after processing according to (10) depends both on the wavelet itself and on the signal shape.

For instance, wavelet db16 for complex signals as Chirps after the mathematical processing using f_{1-3} increases the number of the identification features from 7 to 15, and for the wavelet bior1.1—from 12 to 15. For simple functions, e.g., Blocks, for the wavelet db16, the opposite effect is observed—the number of the identification features decreases from 7 to 1, and for the wavelet bior1.1—from 12 to 1.

Entropy of Shannon, dits
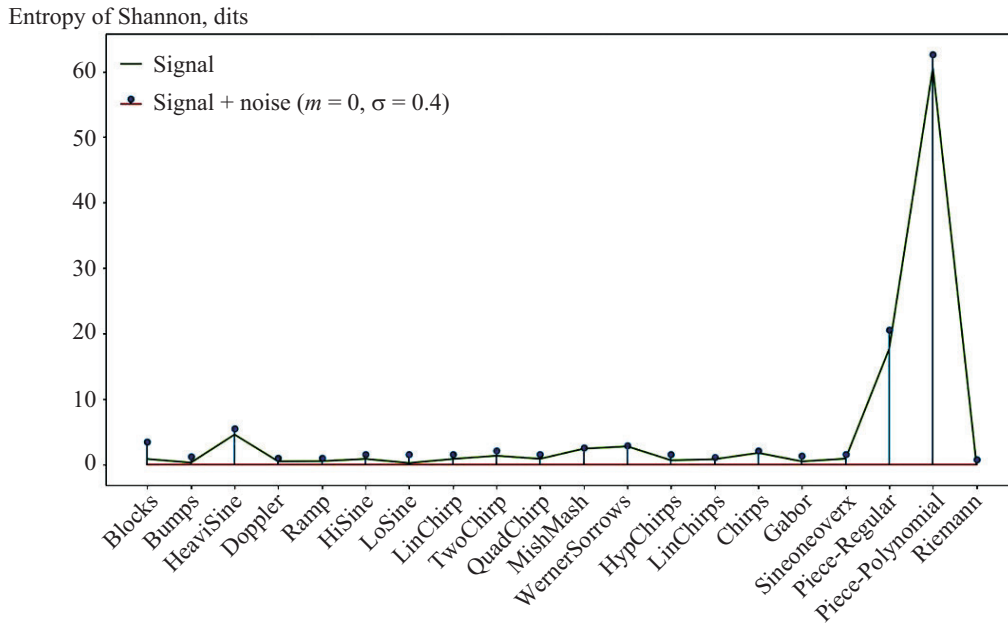
Fig. 1. Signal complexity according to Shannon.
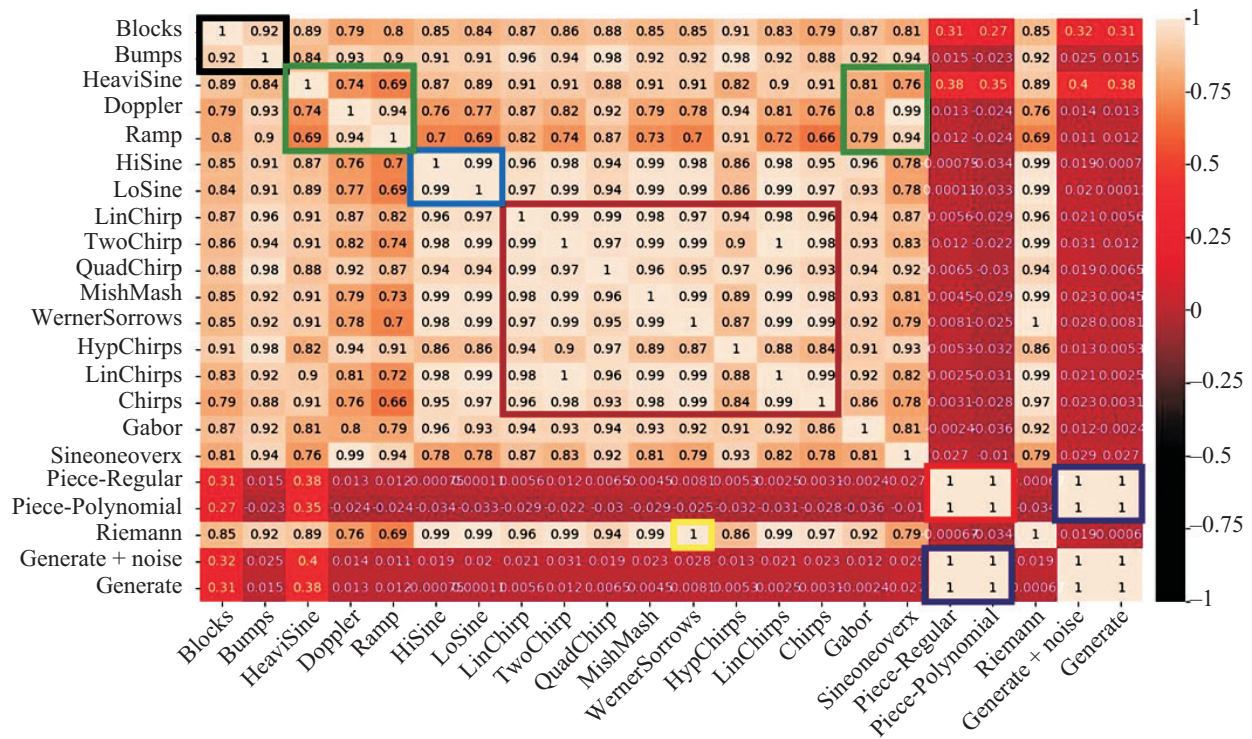
Fig. 2. Correlation matrix of functions from discrete spectra of specific signals.

Let us demonstrate the discussed above by checking not only the visually found signal groups (Tables 1–5) but also their belonging to signal groups (4) from [5]. To do so, we add the white noise with $\sigma = 0.4$ and zero mathematical expectation to the "generate+noise" signal and the "generate" signal without noise. The matrix is built for the db16 wavelet.

Visual analysis of the power of continuous wavelet spectra in a number of groups of signals coincides with the numerical values of the proximity of discrete wavelet spectra. For the Chirps group of signals (Table 3), the area is marked with a red outline. For the HiSine, LoSine group of signals (Table 2), the area is
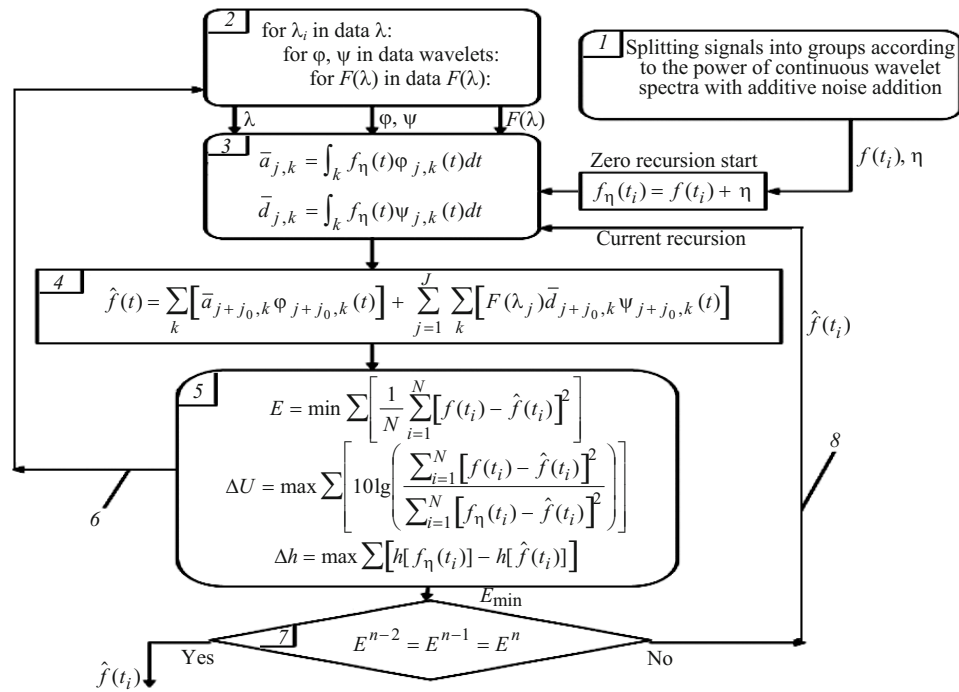
Fig. 3. Algorithm of increasing filtering efficiency by recursion.

marked with a blue outline. The areas showing the similarity of the WernerSorrows and Riemann signals (Table 5) are highlighted in yellow.

The differences between the visual and numerical analysis according to the method proposed by the authors are observed in Table 1. Signals Blocks and Bumps are well correlated with each other (highlighted by the black outline), as well as signals Piece-regular and Piece-polynomial (highlighted in brown). However, there is no correlation between these subgroups. The commonality of the HeaviSine, Doppler, Ramp, Gabor, and Sineoneoverx signals is highlighted by two green contours (Table 4). There are other features that are clearly visible in the recursion graphs given below, intentionally constructed from the results of visual comparison.

The input "generate+noise" and "generate" signals correlate with the Piece-regular and Piece-polynomial signal group. Thus, by mathematical processing of discrete wavelet spectra we have obtained a very significant result. We have replaced the visual comparison of the powers of continuous wavelet spectra with the numerical comparison of functions from discrete spectra. Besides, the resulting matrix has a very high sensitivity to the shape and spectrum of the signal (Fig. 2). It is evidenced by the presence of three "1" outside the diagonal.

6. FILTERING ALGORITHM FOR NOISY SIGNALS

Let us consider an algorithm for increasing the efficiency of DWT filtering with a single threshold for selected groups of signals.

Direct filtration is performed in blocks 2–6 (Fig. 3). In block 2, using the main loop, threshold λ_j for limiting the expansion coefficients is searched, and with the help of two nested loops, the "maternal" ψ and "parent" φ functions of the basic wavelet and the threshold function $F(\lambda_j)$ for limiting the wavelet coefficients are selected.

In block 3 (Fig. 3), noisy signal $f_\eta(t_i) = f(t_i) + \eta$ is decomposed into two sets of wavelet coefficients $\bar{a}_{j,k}$ and $\bar{d}_{j,k}$, where η is the additively added noise. In block 4, using one set of threshold λ_j, wavelet ψ, φ, and threshold function $F(\lambda_j)$ selected in block 2, the noise is suppressed by limiting the detail ratios

$$\sum_{j=1}^{J} \sum_{k} \left[F(\lambda_j) \bar{d}_{j+j_0,k} \psi_{j+j_0,k}(t) \right].$$

Table 6. Comparative efficiency analysis of direct and recursive methods for Group 1

Model function	ΔU, dB	Δh, dit	E^0	Wav	$F(\lambda_j)$	λ_j	n	E^n	Wav^n	$F^n(\lambda_j)$	λ_j^n	$\Delta\%$
Blocks	14	2.4099	0.0214	bior1.1	hard	1.4	14	0.0059	bior1.1	hard	0.2	72.4
Bumps	8	0.8146	0.0363	bior2.8	garotte	1.0	13	0.0267	bior2.8	hard	0.2	26.4
Piece-polynomial	13	2.1828	0.0248	db2	garotte	1.2	14	0.0083	rbio1.3	hard	0.2	66.5
Piece-regular	8	2.1972	0.0429	bior2.4	garotte	0.8	9	0.0255	bior6.8	hard	0.2	40.6

Table 7. Comparative efficiency analysis of direct and recursive methods for Group 2

Model function	ΔU, dB	Δh, dit	E^0	Wav	$F(\lambda_j)$	λ_j	n	E^n	Wav^n	$F^n(\lambda_j)$	λ_j^n	$\Delta\%$
HiSine	3	0.3891	0.1184	sym8	soft	0.2	14	0.0866	db21	hard	0.2	26.9
LoSine	10	0.8788	0.0498	sym16	hard	1.0	13	0.0639	db33	hard	0.2	68.1

The signal is restored in the time domain. In block *5*, through feedback *6* to block *2*, the values of the root-mean-square error

$$\text{RMSE} = \sum \left[\frac{1}{N} \sum_{i=1}^{N} \left[f(t_i) - \hat{f}(t_i) \right]^2 \right]$$

are accumulated. The noise power

$$\sum \left[10\lg \left(\frac{\sum_{i=1}^{N} \left[f(t_i) - \hat{f}(t_i) \right]^2}{\sum_{i=1}^{N} \left[f_\eta(t_i) - \hat{f}(t_i) \right]^2} \right) \right]$$

is reduced, and the entropy of signal

$$\sum \left[h[f_\eta(t_i)] - h[\hat{f}(t_i)] \right]$$

is reduced.

After enumerating all the sets of values from block *2*, the minimum error value $E_{0\min}$ is selected, which is the direct filtering error or zero recursion error. Parameters ΔU and Δh are used for control. Next, the recursion process takes place. The filtered signal enters block *3* many times. The filtering is repeated until the following condition is met:
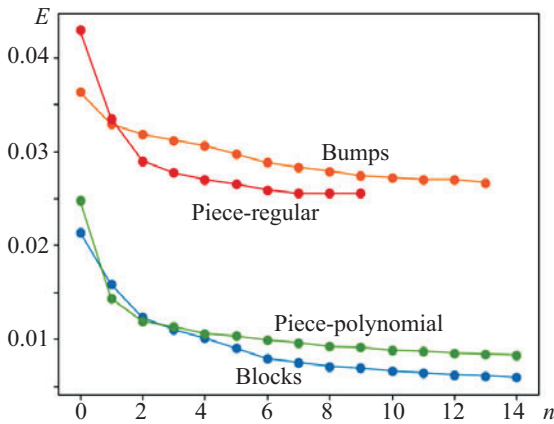
$$E^{n-2} = E^{n-1} = E^n.$$

Fig. 4. Recursive DWT filtration with common threshold for all levels of signal decomposition (Group 1).
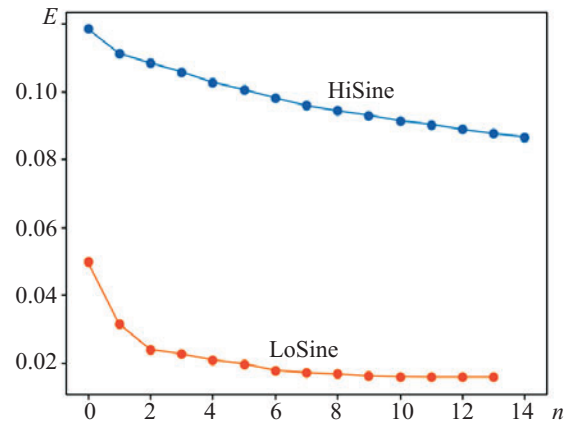

Fig. 5. Recursive DWT filtration with common threshold for all levels of signal decomposition (Group 2).

Each such repetition is called an iteration; it characterizes the efficiency of filtration with the use of recursion by the following parameters: $\Delta = (E_0 - E^n)100/E_0$, ΔU, Δh. It should be noted that this algorithm can be used for a real signal employing the reference signal. In this case, it will be the signal obtained during the first filtering.

7. VERIFICATION OF PROPOSED METHOD

In the simulation, Gaussian uncorrelated noise was used with zero mathematical expectation and the standard deviation of 0.4, by averaging thousands of realizations as [4]. The parameters were calculated according to the methodology [6], using mathematical models for optimizing the computational experiment [15].

In all the tables below, the following designations are used: ΔU is the reduction of the noise power in the filtered signal [dB]; E^0 is the root-mean-square error before recursion, a dimensionless quantity; "Wav" is the name of the basic wavelet that provides the minimum error E^0 before the recursion; $F(\lambda_j)$ is the name of the threshold function providing the minimum error E^0 before the recursion; λ_j is the threshold providing the minimum error E^0 before the recursion (float); n is the number of recursion cycles (integer); E^n, Wav^n, $F^n(\lambda_j)$, λ_j^n are parameters of the discrete wavelet filtering after the recursion; $\Delta\%$ is the reduction of the filtering error after recursion; Δh is the reduction of the entropy of a noisy signal after recursion [dit].

The following signals are considered: Blocks $k = 14/14 = 1.0$, Bumps $k = 8/13 = 0.6150$, Piece-polynomial $k = 13/14 = 0.929$, and Piece-regular $k = 8/9 = 0.889$ dB per iteration (Table 6). In [4], this value is 0.0035 dB per iteration. Thus, the recursion of DWT filtration by the suggested algorithm with the mean value $(1.0 + 0.6150 + 0.929 + 0.889)/(0.0035\times4) = 245$ indicates a higher efficiency of the proposed algorithm, even considering the fact that for the optimal direct preliminary DWT filtering [15], not more than several iterations are spent taking into account the signal shape and the values of the parameter enumeration steps.

The nature of the decrease in the error with the increase of recursion for Group 1 of model functions is shown in the graph (Fig. 4). Here and below, the value of E is given in the MSE format.

Let us conduct a comparative numerical analysis of the data obtained by the authors and the data given in [4] using ratio (3) from the literature review.

Comparative analysis of the data obtained by the authors and the data given in [4] shows that for HiSine signal $k = 0.214$ and for LoSine signal $k = 0.769$ dB per iteration (Table 7). The error E of these functions is presented in Fig. 5. Hence, the mean value is $(0.214 + 0.769)/(0.0035\times2) = 140.4$ that is twice more than in [4].

Comparative analysis of the data obtained by the authors and the data given in [4] shows that for HypChirps signal $k = 1.4$, LinChirp signal $k = 0.2$, LinChirps signal $k = 0.2$, MishMash signal $k = 0.071$,

Table 8. Comparative efficiency analysis of direct and recursive methods for Group 3

Model function	ΔU, dB	Δh, dit	E^0	Wav	$F(\lambda_j)$	λ_j	n	E^n	Wav^n	$F^n(\lambda_j)$	λ_j^n	$\Delta\%$
HypChirps	7	0.6163	0.0371	db31	garotte	0.8	5	0.0311	db35	hard	0.2	16.2
LinChirp	2	0.4633	0.1099	db27	soft	0.4	10	0.0994	sym19	hard	0.2	9.6
LinChirps	5	0.5770	0.0648	db15	soft	0.4	6	0.0573	dmey	less	1.6	11.6
MishMash	1	0.2931	0.1398	db27	soft	0.2	14	0.1261	db23	hard	0.2	9.8
QuadChirp	3	0.3777	0.0825	db32	garotte	0.6	8	0.0727	db38	hard	0.2	11.9
TwoChirp	2	0.3383	0.1333	db19	soft	0.2	14	0.1161	db31	hard	0.2	12.9
Chirps	2	0.3355	0.1166	db30	soft	0.2	10	0.0981	db36	hard	0.2	15.9

Table 9. Comparative efficiency analysis of direct and recursive methods for Group 4

Model function	ΔU, dB	Δh, dit	E^0	Wav	$F(\lambda_j)$	λ_j	n	E^n	Wav^n	$F^n(\lambda_j)$	λ_j^n	$\Delta\%$
Doppler	12	0.5240	0.011	sym12	garotte	1.0	5	0.0094	sym5	hard	0.3	14.5
Gabor	12	0.8953	0.0207	db14	garotte	0.8	14	0.0103	coif9	hard	0.1	50.2
HeaviSine	13	0.9600	0.0146	rbio5.5	garotte	1.0	6	0.0088	bior3.1	hard	0.1	39.7
Ramp	19	0.9600	0.0041	bior1.3	garotte	1.0	4	0.0022	bior1.1	hard	0.1	46.3
Sineoneoverx	9	0.499	0.0278	sym5	garotte	0.8	14	0.0195	bior2.2	hard	0.1	29.9

QuadChirp signal $k = 0.375$, TwoChirp signal $k = 0.143$, and for Chirps signal $k = 0.143$ dB per iteration (Table 8). The error E in this case is shown in Fig. 6. Hence, the mean value is $(1.4+0.2+0.2+0.071+0.375+0.143+0.143)/(0.0035\times7) = 103.3$ that is two times more efficient than in [4].

Comparative analysis of the data obtained by the authors and the data given in [4] shows that for the Doppler signal $k = 2.4$, Gabor signal $k = 0.857$, HeaviSine signal $k = 2.167$, Ramp signal $k = 4.75$, and for the sineoneoverx signal $k = 0.643$ dB per iteration (Table 9). The error E of these functions is presented in Fig. 7. Hence, the mean value is $(2.4 + 0.857 + 2.167 + 4.75)/4 = 2.5435$ that is twice more than in [4].

A comparative analysis of the data obtained by the authors and the data given in [4] shows that for the WernerSorrows signal $k = 0.071$ and Riemann signal $k = 7.333$ dB per iteration (Table 10). The error E in this case is shown in Fig. 8. Hence, the mean value is $(0.071+7.333)/(0.0035\times2) = 1057.7$ that is three times more than in [4].

8. COMPARISON OF RESULTS OBTAINED WITH DATA OF OTHER AUTHORS

Since the recursive DWT algorithm is considered only in one publication [4], the averaged values of the number of iterations per decibel of noise power show advantages of the proposed filtering algorithm (Fig. 3). For the comparative analysis of the filtering error and the data from [5] according to the matrix data in Fig. 2, we introduce a new group of signals: "generate," "Piece-regular," and "Piece-polynomial". The result is shown in Fig. 9.

According to [5], the noise reduction with packet DWT filtering is $20 - 11.1728 = 8.8272$ dB and RMSE $= 0.0147$. For the proposed algorithm, the noise reduction by 15 dB is MSE $= E_4 = 0.0001$ for four iterations. Considering the fact that with MSE $=$ RMSE^2 we get 0.01 that is 0.0047 less.
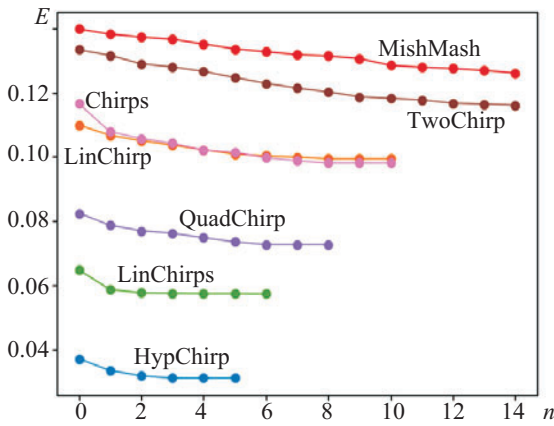
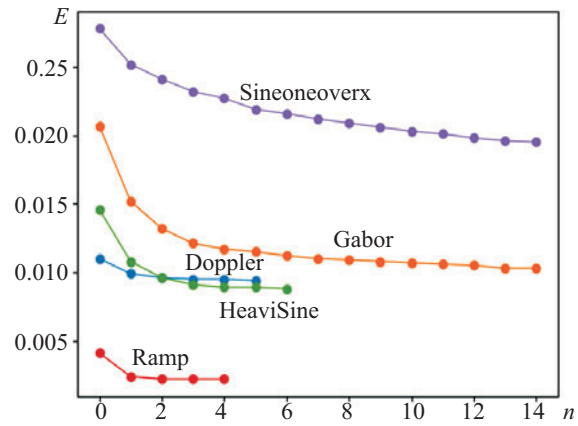**Fig. 6.** Recursive DWT filtration with common threshold for all levels of signal decomposition (Group 3).

Fig. 7. Recursive DWT filtration with common threshold for all levels of signal decomposition (Group 4).

Table 10. Comparative efficiency analysis of direct and recursive methods for Group 5

Model function	ΔU, dB	Δh, dit	E^0	Wav	$F(\lambda_j)$	λ_j	n	E^n	Wav^n	$F^n(\lambda_j)$	λ_j^n	$\Delta\%$
Riemann	1	0.1459	0.1459	sym19	soft	0.1	14	0.1361	db26	hard	0.1	6.7
WernerSorrows	22	0.8057	0.0013	bior1.1	soft	1.0	3	0.001	bior2.2	garotte	0.1	23.1

9. PRACTICAL VALUE OF RESULTS

The algorithm presented above allows us to use the recursion without a model function and in case of the real signal taking the first filtering as the original signal. This is especially important for a group of Chirps signals which are used in many applications [8]–[11]. For example, in radars the reduction of the error from barrage noise by 10% can significantly extend the viability of unmanned aerial vehicles. Moreover, the numerical identification of signals into groups simplifies their identification and has a simple software implementation.

The scientific novelty of the publication lies in the fact that for the discrete DWT in accordance with the algorithm in Fig. 3, the recursion can be applied that increases its efficiency.

10. CONCLUSIONS

It is shown that, due to the choice of a discrete wavelet and special mathematical functions for processing wavelet coefficients, the correlation matrix provides a high selectivity not only for groups of signals of similar shape, but also for an individual signal. Mathematical functions for processing wavelet coefficients are divided into two groups. According to numerical values of the Shannon entropy, the signals can be conditionally divided into simple and complex.

The first group of statistics consists of ten functions, including variance, standard deviation, mean value, the 5th, 25th, 75th, 95th percentile values, root mean square value, and the squared root mean square amplitude. This group of functions solves the problem of identifying simple signals.

The second group is designed to detect crossover signals with linear and nonlinear frequency modulation. These include the average value of the derivative, the frequency of zero-crossing, and the average speed of transition of the given signal amplitude.

Groups of mathematical functions for processing wavelet coefficients do not depend on each other. Hence, this set is acceptable both for conditionally simple and conditionally complex signals.

The frequency correlation matrix of test signals in the form of functionally processed wavelet coefficients is stored in the database and is extended when new signals are detected. The selectivity of the frequency matrix also depends on the number of identification features. The dependence of the number of
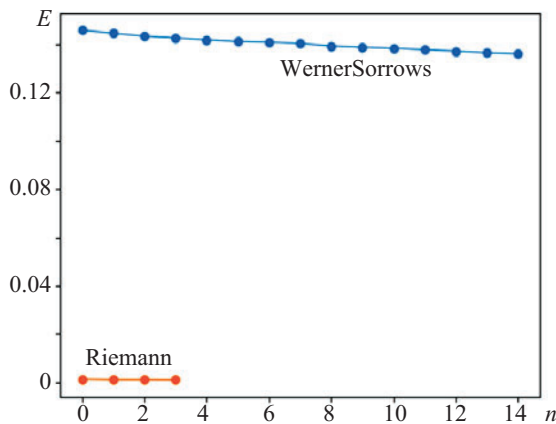
Fig. 8. Recursive DWT filtration with common threshold for all levels of signal decomposition (Group 5).
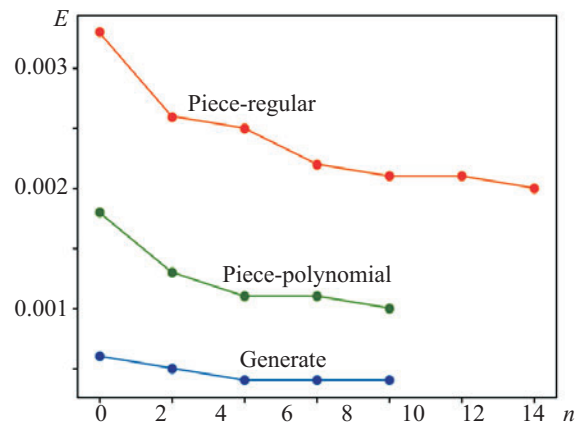
Fig. 9. Comparison of suggested algorithm with [5].

identification features on the signal length and the type of discrete wavelet is found. This allows determining the wavelet at which the sensitivity of the frequency correlation matrix is maximum for signals of the same length.

The real signal contains a noise component. The correlation matrix makes it possible to identify noisy signals. After identifying the real signal using tabular data about the main wavelet, threshold, threshold function, the recursive filtering should be performed to remove noise. If the noise error for the identified signal is reduced compared to the known data, wavelet filtering of the real signal is performed without using a model function directly. A comparative analysis of the obtained results and the known data shows a sufficient efficiency of the proposed algorithm in terms of both the noise reduction per iteration and the final value of the root- mean-square error.

CONFLICT OF INTEREST

The authors declare that they have no conflicts of interest.

ADDITIONAL INFORMATION

REFERENCES

1. Y. N. Klikushin and V. Y. Kobenko, "Fundamentals of identification measurements," *Radio Electron. J.*, No. 5 (2006). URL: http://jre.cplire.ru/iso/nov06/index.html.
2. A. K. Lagirvandze, A. N. Kalinichenko, and T. V. Morgunova, "ECG cycles forms analysis based on machine learning techniques," *Model. Syst. Networks Econ. Technol. Nature, Soc.*, No. 4, 75 (2019).
3. D. A. Kuzin, L. G. Statsenko, P. N. Anisimov, and M. M. Smirnova, "Applying machine learning methods to acoustic signal classification using spectrum characteristics," *Izv. SPBGETU "LETI"*, No. 3, 48 (2021).
4. M. S. Salman, A. Eleyan, and B. Al-Sheikh, "Discrete-wavelet-transform recursive inverse algorithm using second-order estimation of the autocorrelation matrix," *TELKOMNIKA* (*Telecommunication Comput. Electron. Control.* **18**, No. 6, 3073 (2020). DOI: 10.12928/telkomnika.v18i6.16191.
5. T. Hu, J. Zhao, S. Yan, and W. Zhang, "Performance analysis of a wavelet packet transform applied to concrete ultrasonic detection signals," *J. Phys. Conf. Ser.* **1894**, No. 1, 012062 (2021). DOI: 10.1088/1742-6596/1894/1/012062.
6. V. O. Braun, V. P. Dolgushin, V. N. Loza, and I. V. Pampukha, "Investigation of possibilities and characteristics of methods for reducing noise level in signal processing based on use of wavelet technology," *Radio Electron. J.*, No. 7 (2014). URL: http://jre.cplire.ru/jre/jul14/6/text.html.
7. Y. K. Taranenko, V. V. Lopatin, and O. Y. Oliynyk, "Wavelet filtering by using nonthreshold method and example of model Doppler function," *Radioelectron. Commun. Syst.* **64**, No. 7, 380 (2021). DOI: 10.3103/S0735272721070049.

8. G. Galati, G. Pavan, and F. De Palo, "Chirp signals and noisy waveforms for solid-state surveillance radars," *Aerospace* **4**, No. 1, 15 (2017). DOI: 10.3390/aerospace4010015.

9. D. O. Hogenboom and C. A. DiMarzio, "Quadrature detection of a Doppler signal," *Appl. Opt.* **37**, No. 13, 2569 (1998). DOI: 10.1364/AO.37.002569.

10. L. Debnath, "The Gabor Transform and Time-Frequency Signal Analysis," in *Wavelet Transforms And Their Applications* (Birkhäuser Boston, Boston, MA, 2002), pp. 257–306. DOI: 10.1007/978-1-4612-0097-0_4.

11. M. Kovacević, "Signaling to relativistic observers: an Einstein–Shannon–Riemann encounter," *Probl. Inf. Transm.* **56**, No. 4, 303 (2020). DOI: 10.1134/S0032946020040018.

12. P. Virtanen, R. Gommers, T. E. Oliphant, M. Haberland, T. Reddy, D. Cournapeau, E. Burovski, P. Peterson, W. Weckesser, J. Bright, S. J. van der Walt, M. Brett, J. Wilson, K. J. Millman, N. Mayorov, A. R. J. Nelson, E. Jones, R. Kern, E. Larson, *et al.*, "SciPy 1.0: fundamental algorithms for scientific computing in Python," *Nat. Methods* **17**, No. 3, 261 (2020). DOI: 10.1038/s41592-019-0686-2.

13. S. K. Goh, H. A. Abbass, K. C. Tan, A. Al-Mamun, C. Wang, and C. Guan, "Automatic EEG artifact removal techniques by detecting influential independent components," *IEEE Trans. Emerg. Top. Comput. Intell.* **1**, No. 4, 270 (2017). DOI: 10.1109/TETCI.2017.2690913.

14. B. Belkacemi, S. Saad, Z. Ghemari, F. Zaamouche, and A. Khazzane, "Detection of induction motor improper bearing lubrication by discrete wavelet transforms (DWT) decomposition," *Instrum. Mes. Métrologie* **19**, No. 5, 347 (2020). DOI: 10.18280/i2m.190504.

15. Y. K. Taranenko, "Methods of discrete wavelet filtering of measuring signals: an algorithm for choosing a method," *Izmer. Tekhnika*, No. 10, 14 (2021). DOI: 10.32446/0368-1025it.2021-10-14-20.